

First quantum machine learning applications on an on-site room-temperature quantum computer

Nils Herrmann,* Daanish Arya, Florian Preis,[†] and Stefan Prestel
Quantum Brilliance GmbH
Colorado Tower Industriestr. 4
70565 Stuttgart, Germany

Mariam Akhtar, Marcus W. Doherty, Pascal Macha, and Michael L. Walker
Quantum Brilliance Pty Ltd
60 Mills Road
Acton ACT 2601, Australia
(Dated: December 20, 2023)

We demonstrate – for the first time – the application of a quantum machine learning (QML) algorithm on an on-site room-temperature quantum computer. A two-qubit quantum computer installed at the Pawsey Supercomputing Centre in Perth, Australia, is used to solve multi-class classification problems on unseen, i.e. untrained, 2D data points. The underlying 1-qubit model is based on the data re-uploading framework of the universal quantum classifier [1] and was trained on an ideal quantum simulator using the Adam optimiser [2]. No noise models or device-specific insights were used in the training process. The optimised model was deployed to the quantum device by means of a single XYX decomposition leading to three parameterised single qubit rotations. The results for different classification problems are compared to the optimal results of an ideal simulator. The room-temperature quantum computer achieves very high classification accuracies, on par with ideal state vector simulations.

I. INTRODUCTION

Machine learning (ML) is a highly anticipated sub-field of artificial intelligence (AI) that aims to find or “learn” optimised models without explicit instructions [7]. The aim is to create models that can effectively predict or classify examples outside the training data in problems where the underlying mathematical correlations are either unknown or too complex for conventional approaches. Here, special care needs to be taken to compile training data sets that ensure a sufficiently general model [8]. Especially in light of the newly developed generative ML models, such as the GPT-4 large language model [9], concerns have been raised addressing their increasing training demands both in energy consumption and carbon footprint [10, 11]. The advent of quantum computing has created high hopes for the field of ML by utilising the exponentially growing n -qubit Hilbert space as the addressable feature space in ML pipelines. Recently, it has been shown that quantum ML (QML) methods are capable to efficiently generalise from fewer training data [12], can achieve better prediction accuracies [13], and possess an inherent advantage in handling quantum data [14] compared to their classical competitors, sparking hopes to arrive at a practical quantum advantage – recently coined as Quantum Utility [15].

Schuld and Petruccione [3] separated QML methods into four distinct categories as shown in subfigure 1a. [10, 11] Here, CC refers to approaches where classical

data is processed using classical algorithms. This includes standard classical ML approaches but in the context of QML refers to those using only quantum-inspired classical algorithms such as tensor network methods. These have recently been used to train ML methods affected by the big data problem in high-energy physics [16]. The QC category involves QML methods that learn from quantum data and apply classical algorithms. Prominent examples include ML-based quantum state tomography [17] and classically distinguishing between quantum states [18, 19]. Of most interest, in the pursuit of Quantum Utility [15], are the CQ and QQ methods, which learn from either conventional or quantum data and train a quantum model, typically a parameterised quantum circuit. Tremendous advances in this field have been reported in the literature over the last years. For an extensive review of current QML advances, please refer to references [20–24].

In this work, we focus on the CQ sector of QML applications and present – for the first time – results of a quantum classification model from a quantum computer operating at standard ambient conditions (room temperature and standard pressure) on-site a data centre for high performance computing. The model is based on the Universal Quantum Classifier (UQC) [1]. Very recently, there have been reports of successful applications of the UQC method on ion trap [25], photonic [26], and superconducting [27] architectures. All deployed models reach classification accuracies above 90%, on par or better than classical competitors with a similar number of trainable parameters [28]. The results, reported in this work, differ from the already published applications in two fundamental points:

* nils.herrmann@quantum-brilliance.com

[†] f.preis@quantum-brilliance.com

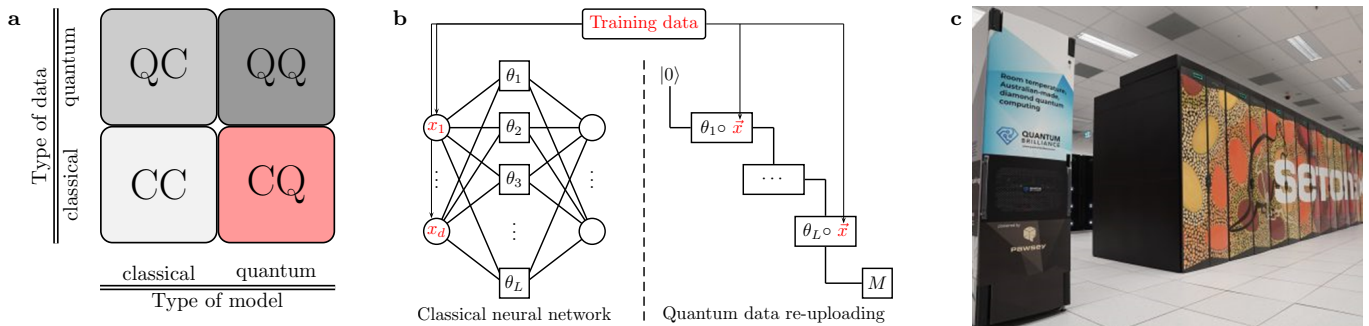


Figure 1: The first QML application on an on-site room-temperature quantum computer **1a** Following Schuld and Petruccione [3], the field of quantum machine learning (QML) is separable into four distinct categories. In this work, we focus on classical data processed by a quantum model (“CQ”, highlighted in red). **1b** The applied model – the Universal Quantum Classifier (UQC) [1] – is based on the data re-uploading framework [1], which effectively circumvents the no-cloning theorem [4–6], creating an analogy between single-layered classical neural networks and single qubit quantum circuits. **1c** After having obtained classically trained UQC models, different classification problems were solved using the Quantum Brilliance Quantum Development Kit (QB-QDK) – an on-site room-temperature quantum computer installed at the Pawsey Supercomputing Centre in Perth, Australia.

- (i) All results in this study were obtained from an on-site nitrogen-vacancy-based spin qubit quantum computer, operating at ambient conditions and mounted on a standard 19” HPC server rack in the Pawsey Supercomputing Centre.
- (ii) The native performance of the quantum computer was sufficient to achieve high classification accuracies from classically trained (on an ideal simulator using classical hardware) quantum models without the need for additional noise mitigation techniques or on-device training.

Therefore, this work marks an important milestone in the pursuit of Quantum Utility [15]. Tackling more complicated and classically difficult classification problems using larger UQC models with more trainable parameters will ultimately require large quantum processing resources. Here, a simple but robust integration to classical computing centres as demonstrated with point (i), will enable massively parallel diamond quantum infrastructures, accelerating the UQC training by the parallel distribution of workflows [29]. At the same time, the trained models remain executable on individual diamond quantum processing units, which – due to their ability to operate in ambient conditions – are edge-deployable. Given a sufficient native device performance, these individual units could be used to perform highly complicated inference tasks utilising feature space mappings inaccessible by even the largest classical computing facilities. Following a similar train of thought and indicated by point (ii), it might even be possible to achieve Quantum Utility by larger but classically trained UQC models. Here, moderately-sized UQC models could be trained on large supercomputing infrastructures and then deployed to individual on-site diamond quantum processing units. If the latter are able to outperform classical processing units of similar size, weight, and cost by being faster,

more accurate, or requiring less energy [15], a practical quantum advantage could be achieved in the near future.

The paper is structured as follows: Section II briefly summarises the theory behind the UQC model, while section III focuses on the application details covering the classical training process in subsection III A, the circuit offloading to the quantum processing unit (QPU) in subsection III B as well as the integration and installation of the quantum device itself in subsection III C. Section IV highlights the classification results for binary and trinary classification problems of two-dimensional classical data, and compares to an ideal state vector quantum simulator.

II. ALGORITHMIC DETAILS

The Universal Quantum Classifier [1] is based on the data re-uploading framework, effectively circumventing the no-cloning theorem [4–6] of quantum computing. This allows the direct correspondence between a single-layered classical neural network and a parameterised single qubit quantum circuit shown in Figure 1b.

In a single layered classical neural network, the training data \vec{x} is (i) passed on to all connected processing nodes of the hidden layer, (ii) processed according to the individual activation functions, and then (iii) re-collected in single or multiple output nodes. The parameters or weights $\theta_1, \dots, \theta_L$ are optimised with respect to a global cost function. All data connections are applied in parallel, effectively requiring a parallel copy operation, which is inherently impossible on quantum computers [4–6]. Pérez-Salinas et al. [1] proposed to circumvent this problem by serializing all processing nodes into parameterised consecutive quantum gates $\theta_1 \circ \vec{x}, \dots, \theta_L \circ \vec{x}$, where the input data \vec{x} is re-uploaded in every single step before the final result is extracted from a final measurement M . The parameters $\theta_1, \dots, \theta_L$ may be optimised

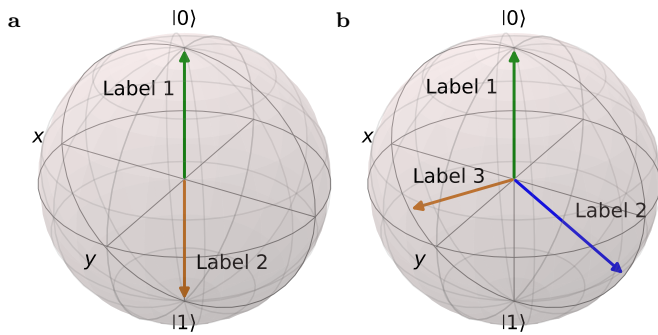


Figure 2: Mapping of classification labels c to maximally orthogonal state vectors $|Y_c\rangle$. The binary and trinary classification labels c in this work, were mapped to maximally orthogonal label states Y_c on the surface of the single qubit Bloch sphere. This allowed a straightforward association of measured quantum densities to classification labels by means of the respective quantum state fidelity. The label states used in this work are shown in subfigures 2a and 2b, respectively.

classically according to a global cost function in a hybrid classical-quantum algorithm pipeline. In contrast to the classical single layered neural network, two major observations can be made:

- (I) Despite being applied within a single qubit circuit, the unitary product of all parameterised and re-uploaded gates may introduce highly (up to order L) non-linear terms in regard to the input data \vec{x} possibly leading to a much better feature space mapping than accessible by the single layered neural network.
- (II) While the classically trivial part of the neural network, i.e. the parallel data distribution, needs to be serialised on the qubit register, the classically hard part, i.e. the realisation of deep neural networks with many hidden layers, may be much simpler in the quantum circuit. By extending the 1-qubit data re-uploading circuit to n qubits with additional entangling layers in between the re-uploads, one may arrive at a natural augmentation to “quantum deep learning” [1].

To apply the data re-uploading framework to a multi-label classification task, the measurement outputs need to be mapped to the individual classification labels. This can be achieved using maximally orthogonal label states $|Y_c\rangle$ for each classification label c as shown in Figure 2 for binary (subfigure 2a) and trinary (subfigure 2b) classification tasks.

The classification label c may be acquired by measuring the single qubit state tomography after applying the full data re-uploading circuit and identifying the closest mapped label state $|Y_c\rangle$ to the measured density $\tilde{\rho}(\vec{\theta}, \vec{x}_\mu)$, i.e. identifying $|Y_c\rangle$ with the largest fidelity to $\tilde{\rho}(\vec{\theta}, \vec{x}_\mu)$.

The circuit parameters may then be trained in a supervised learning algorithm to move the single qubit states as close as possible to their respective label states depending on the uploaded input data \vec{x} . Given that the final classification result is based on a fidelity metric, the UQC pipeline is naturally robust to quantum noise [30]. Given an optimal set of circuit parameters, noise will affect the classified labels if and only if the measured density gets closer to another, i.e. wrong, maximally orthogonal label state. In other words, binary classification results will remain accurate as long as noise does not shift the measured densities to the wrong hemisphere on the Bloch sphere. Analogous reasoning applies to multi-label classification problems, where each additional label state decreases the overall noise tolerance.

For the actual training process, a straightforward cost function $\chi_f^2(\vec{\theta})$ with

$$\chi_f^2(\vec{\theta}) = \sum_{\mu=1}^{|T|} \left(1 - \langle Y_{c(\mu)} | \tilde{\rho}(\vec{\theta}, \vec{x}_\mu) | Y_{c(\mu)} \rangle \right) \quad (1)$$

is based on the quantum state fidelity $\langle Y_{c(\mu)} | \tilde{\rho}(\vec{\theta}, \vec{x}_\mu) | Y_{c(\mu)} \rangle$ of the (pure) label state $|Y_{c(\mu)}\rangle$ of the correct label $c(\mu)$ of training data point \vec{x}_μ and the measured density $\tilde{\rho}(\vec{\theta}, \vec{x}_\mu)$. Clearly, the cost function approaches zero if all training data points of the training data set T lead to quantum states coinciding with exact label states.

III. METHODS

A. Training process

Three different two-dimensional data sets were used in the training process of the UQC model. All sets contained data points in \mathbb{R}^2 within the boundaries of $[-1, +1]$ and were generated using a random number generator. For each data point, labels were generated based on separating margins set by

- (i) a single circle of radius $\sqrt{\frac{2}{\pi}}$ centred at $(0, 0)$,
- (ii) the sine function $s(x) = \frac{8}{10} \sin(\pi x)$, and
- (iii) two circles of radii 1 and 0.4 centred at $(-1, -1)$ and $(0.3, 0.3)$, respectively.

For training and validation, two data sets composed of 1,000 and 2,000 data points, respectively, were generated. The training was performed in batches of 100 data points using the Adam optimiser [2] employing 20 epochs and a learning rate of 0.6, as well as $\beta_1 = 0.9$ and $\beta_2 = 0.999$. The trained UQC model consisted of parameterised arbitrary rotation gates repeatedly employing unitaries

$$U_l = R(\vec{v}^{(l)}) = R_Z(v_3^{(l)}) R_Y(v_2^{(l)}) R_Z(v_1^{(l)}) \quad (2)$$

with

$$\vec{v}^{(l)} = \begin{pmatrix} v_1^{(l)} \\ v_2^{(l)} \\ v_3^{(l)} \end{pmatrix} = \vec{\theta}^{(l)} \circ \vec{x} + \vec{\omega}^{(l)} = \begin{pmatrix} \theta_1^{(l)} x_1 + \omega_1^{(l)} \\ \theta_2^{(l)} x_2 + \omega_2^{(l)} \\ \omega_3^{(l)} \end{pmatrix} \quad (3)$$

for layers $l = 1 \dots L$. The two-dimensional input data \vec{x} used in this work implies that each layer U_l involves five trainable parameters (two $\theta^{(l)}$ and three $\omega^{(l)}$). Six layers were used for the binary and ten layers for the trinary classification problems, resulting in 30 and 50 trainable parameters, respectively. During the optimisation, the fidelity-based cost function (1) was minimised. All quantum circuits involved in the training process were evaluated classically and off-site using an ideal state vector simulator.

B. Deployment to the quantum device

After obtaining a trained model in the form of optimised rotation angles $\vec{\theta}^{(l)}$ and $\vec{\omega}^{(l)}$, new random data points were (i) generated, (ii) inserted into the circuit model, and (iii) classically transpiled into a single sequence of XYX rotations to be deployed to our room-temperature quantum computer – the Quantum Development Kit (QB-QDK). A schematic pictogram displaying the deployment route is shown in Figure 3.

Since the product of two unitaries remains unitary, it is possible to condense all re-uploading layers $1 \dots L$ into a single unitary $U_1 \cdot U_2 \dots U_L$, which can then be decomposed (while neglecting an irrelevant global phase) into three single qubit rotations R_X , R_Y , and R_X , which are part of the native gate set of the QB-QDK. Note that no approximations are involved, such that the final condensed circuit still reflects an exact implementation of the classically optimised data re-uploading circuit. Such simplification techniques are possible due to the limited width of the circuit, but would incur significant overhead in a scaled-up version of the UQC (e.g. for 30+ qubits). Our results may nevertheless provide a valuable milestone in room-temperature quantum computing because

- (i) the deployed models were trained entirely on an ideal state vector simulator, allowing us to directly assess the performance of the QB-QDK against the ideal (noise-free) performance,
- (ii) the QB-QDK was operating under real-world conditions in a supercomputing centre, i.e. mounted in a HPC server rack experiencing all environmental disturbances such as acoustical and vibrational noise, high temperatures, high air movement, and strong electromagnetic field interference (a detailed performance analysis will be published separately [31]),
- (iii) no noise mitigation techniques were applied to the measured bit counts.

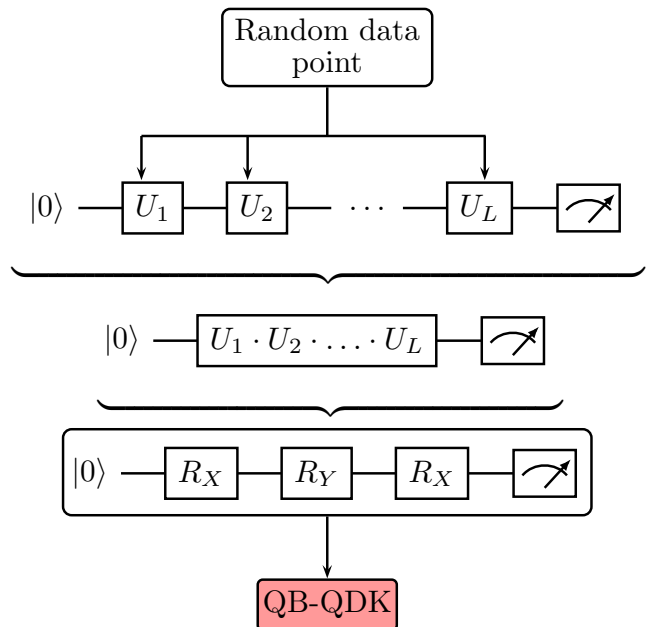


Figure 3: Schematic deployment pipeline of classically optimised UQC models to the QB-QDK quantum computer. To execute inference tasks on the QB-QDK, unseen randomly generated data points were uploaded into the classically optimised UQC models, transpiled into a single sequence of $R_X R_Y R_X$ rotations and sent off to the room-temperature quantum computer (highlighted in red).

To measure inference of the classically optimised UQC models on the QB-QDK, the condensed XYX circuits were offloaded to the control system of the QB-QDK and measured for 100 shots for each data point and measurement basis. In case of the binary classification problems, a single measurement in the computational basis was sufficient to estimate the classification label, i.e. distinguish between upper and lower Bloch hemispheres (cf. Figure 2a). Trinary classification problems, required an additional measurement basis orthogonal to the computational basis to estimate the two-dimensional projection of the full Bloch vector to the respective label state plane (cf. Figure 2b).

C. Integration and set up of the quantum device

The QB-QDK is a 19 inch rack-mounted prototype system featuring a room-temperature quantum processing unit (QPU) with 2 qubits built by Quantum Brilliance. The quantum system is based on a diamond nitrogen-vacancy (NV) centre and consists of one electronic spin associated with the lattice vacancy and an intrinsic ^{14}N as well as an adjacent ^{13}C atom [32]. The nuclear spin states are used to form the qubit states.

This work has been performed on a unit in the Pawsey Supercomputing Centre server room. For ease of inte-

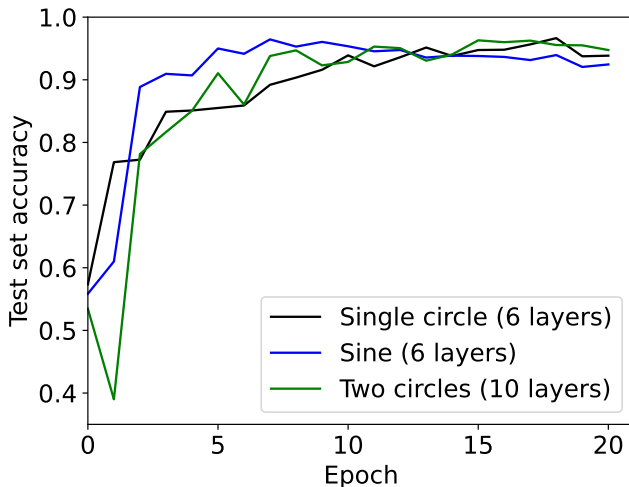


Figure 4: Training performance of the simulated UQC model. In every training epoch of each UQC model, their performance was validated against a test data set of 2,000 randomly generated data points. This figure shows the achieved classification accuracy per training epoch and UQC model. For the two binary and the trinary classification problems, six and ten circuit layer repetitions were used, respectively.

gration, the system’s form factor (44.5 cm, 31 cm and 76 cm for the width, height and depth respectively) complies with standard server rack specifications. An image of the quantum computer in the supercomputing centre server room can be seen in Figure 1c. The overall power consumption is approximately 180 W and is provided by a single mains power cable. The only other external connection is a gigabit fibre connection to the Pawsey networking system, which allows the system to receive pre-compiled circuits in its native gate set (R_X , R_Y , CZ). The QPU is being kept operational by an automatic calibration system, and is interfaced by the full-stack quantum control system developed by Quantum Brilliance. Gate operations are implemented using a series of microwave and radio-frequency pulses, that are applied to the NV in the presence of a DC magnetic field [32].

IV. RESULTS

The classification accuracy for the balanced test data set during the training process is displayed in Figure 4 for the UQC simulated on an ideal state vector simulator for the binary circle and sine problems and the trinary two circle problem.

Although the UQC model was trained using small batches of 100 training data points, its test set performance increased quickly within the first few epochs. Independent of the classification problem, optimal test set accuracies above 90% were reached already within the first ten training epochs. There are no qualitative dif-

ferences between the training performances of the binary (six layers, 30 parameters) and the trinary (ten layers, 50 parameters) UQC models. In both cases, the UQC model could be trained efficiently from small training data batches.

Figure 5 shows the classification results of (i) the UQC executed on an ideal simulator, and (ii) the UQC circuits deployed to the on-site room-temperature quantum computer QB-QDK.

New, randomly generated data points were used to validate the performance for each classification problem. These are shown as individual points in the respective plots. For the binary and trinary classification problems, 200 and 150 data points requiring 20,000 and 30,000 measurements, respectively, were evaluated. The colour of the data points represents the classification result (label) returned by the respective models. The separating margins imposed by the training data are included as only a visual aid.

The UQC model could effectively learn all defining features of the training data sets, reaching excellent classification accuracies of 0.95, 0.97, and 0.873 and 0.925, 0.955, and 0.850 on the ideal state vector simulator and the QB-QDK, respectively. Please note that the optimised classification accuracy of the UQC model was above 0.9 for the much larger test data set of the two circle problem (cf. Figure 4). The specific selection of 150 random data points in Figure 5 lead to a slightly lower performance. In comparison to the ideal state vector results, the QB-QDK performed surprisingly well, almost reaching the exact limit of the ideal state vector simulation in terms of the classification accuracy. Overall, the QB-QDK reached only 1.5% to 2.5% lower classification accuracies. Especially in light of the fact that no on-device training was necessary before deploying the UQC circuits to the QB-QDK (cf. subsection III B), these results indicate a significant milestone in room-temperature quantum machine learning in the prospect of Quantum Utility [15].

Due to quantum noise, a few central data points were seriously misclassified (e.g. the two orange data points near the centre of the upper right circle in the two circle data set). Such effects could lead to problems in time-constrained QML applications. However, it is reasonable to assume that such effects decrease as the performance of the quantum device is optimised. Improved initialisation, gate, and readout fidelities will ultimately lead to better classification accuracies, approaching the classical limit set by exact state vector simulations.

V. CONCLUSION

In this work, the first QML applications deployed to an on-site quantum computer operating at ambient conditions (room temperature and ambient pressure) – the QB-QDK – were reported. The UQC model based on the data re-uploading framework was trained on an ideal

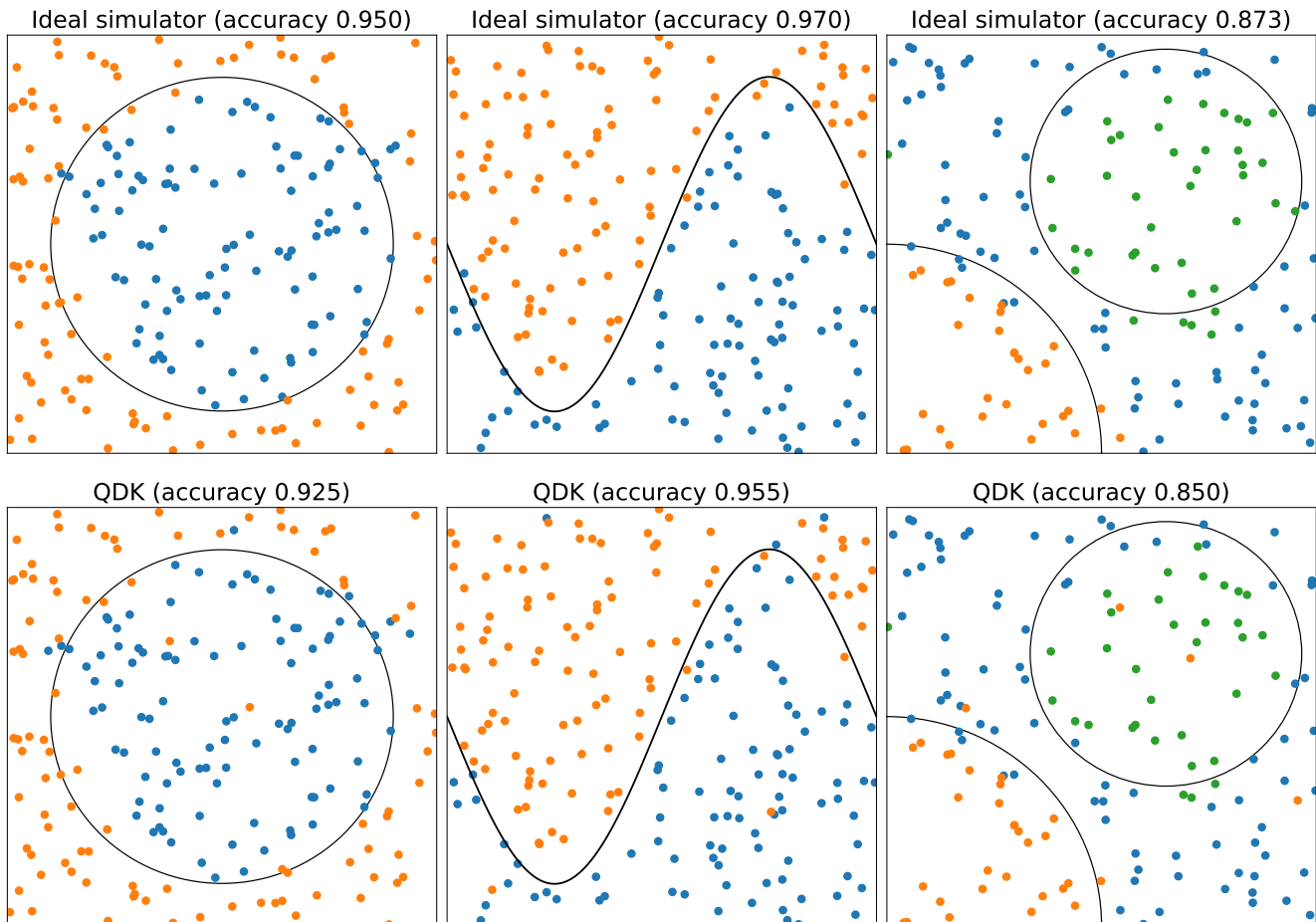


Figure 5: Classification results of the trained UQC models. The results for each classification problem obtained from inference of the trained UQC models on an ideal state vector simulator (top) as well as deployed to an on-site room-temperature quantum computer, i.e. the QB-QDK (bottom). Each data point is coloured according to the obtained classification label. Separating margins are explicitly shown as a visual aid, only.

state vector simulator. Subsequently, the optimised circuits were offloaded to real quantum hardware to infer the labels of newly generated data points. The classification results were compared to the exact limit obtainable by ideal state vector simulations.

The main results collected in Figures 4 and 5 reveal that

- (i) the UQC model was able to efficiently learn the defining features of the training data sets,
- (ii) the UQC model could be trained in small training data batches, converging to optimal test set classification accuracies within the first 10 epochs,
- (iii) no on-device training or noise mitigation techniques were required to successfully deploy the classically optimised models to the integrated quantum hardware, reaching classification accuracies only 1.5% to 2.5% lower than what is possible with ideal state vector simulators.

Item (iii) marks an important milestone for room-temperature quantum computing, paving a promising

path towards Quantum Utility [15] in the real world: Intermediate sized QML models are trained on large HPC or massively parallel quantum infrastructures and then deployed to single on-site quantum accelerators to perform highly complicated inference tasks. Provided such tasks are able to outperform similar classical devices in terms of size, weight, and cost in regard to either total runtime, accuracy, or energy demands, the first practical application of quantum computers could be realised.

ACKNOWLEDGEMENT

The authors would like to thank the Pawsey Supercomputing Centre for their support hosting and integrating the first on-premises room-temperature quantum computer. In particular, we would like to thank Maciej Cytowski, Marco De La Pierre and Ugo Varetto for the fruitful collaboration and the invaluable feedback. The authors would also like to acknowledge funding by the BMBF, in particular projects SPINNING

(FKZ 13N16220), QC4DB (FKZ 13N16091), and QuantumQAP (FKZ: 13N16233).

-
- [1] Adrián Pérez-Salinas, Alba Cervera-Lierta, Elies Gil-Fuster, and José I. Latorre. Data re-uploading for a universal quantum classifier. *Quantum*, 4:226, 2020.
- [2] Diederik P. Kingma and Jimmy Ba. Adam: A method for stochastic optimization. arXiv:1412.6980, 2017.
- [3] Maria Schuld and Francesco Petruccione. *Machine Learning with Quantum Computers*. Quantum Science and Technology. Springer Cham, 2nd edition, October 2021.
- [4] James L. Park. The concept of transition in quantum mechanics. *Found. Phys.*, 1:23, 1970.
- [5] W. K. Wootters and W. H. Zurek. A single quantum cannot be cloned. *Nature*, 299:802, 1982.
- [6] D. Dieks. Communication by epr devices. *Phys. Lett. A*, 92:271, 1982.
- [7] Christian Janiesch, Patrick Zschech, and Kai Heinrich. Machine learning and deep learning. *Electron. Mark.*, 31:685, 2021.
- [8] Mehryar Mohri, Afshin Rostamizadeh, and Ameet Talwalkar. *Foundations of Machine Learning*. The MIT Press, Cambridge, Massachusetts, 2nd edition, 2018.
- [9] OpenAI. Gpt-4 technical report. arXiv:2303.08774, 2023.
- [10] David Patterson, Joseph Gonzalez, Quoc Le, Chen Liang, Lluís-Miquel Munguia, Daniel Rothchild, David So, Maud Texier, and Jeff Dean. Carbon emissions and large neural network training. arXiv:2104.10350, 2021.
- [11] Alex de Vries. The growing energy footprint of artificial intelligence. *Joule*, 7:2191, 2023.
- [12] Matthias C. Caro, Hsin-Yuan Huang, M. Cerezo, Kunal Sharma, Andrew Sornborger, Lukasz Cincio, and Patrick J. Coles. Generalization in quantum machine learning from few training data. *Nat. Commun.*, 13:4919, 2022.
- [13] Nimish Mishra, Manik Kapil, Hemant Rakesh, Amit Anand, Nilima Mishra, Aakash Warke, Soumya Sarkar, Sanchayan Dutta, Sabhyata Gupta, Aditya Prasad Dash, Rakshit Gharat, Yagnik Chatterjee, Shivarati Roy, Shivam Raj, Valay Kumar Jain, Shreeram Bagaria, Smit Chaudhary, Vishwanath Singh, Rituparna Maji, Priyanka Dalei, Bikash K. Behera, Sabyasachi Mukhopadhyay, and Prasanta K. Panigrahi. Quantum machine learning: A review and current status. In *Data Management, Analytics and Innovation*, page 101, Singapore, 2021. Springer Singapore.
- [14] Hsin-Yuan Huang, Michael Broughton, Jordan Cotler, Sitan Chen, Jerry Li, Masoud Mohseni, Hartmut Neven, Ryan Babbush, Richard Kueng, John Preskill, and Jarrod R. McClean. Quantum advantage in learning from experiments. *Science*, 376:1182, 2022.
- [15] Nils Herrmann, Daanish Arya, Marcus W. Doherty, Angus Mingare, Jason C. Pillay, Florian Preis, and Stefan Prestel. Quantum utility – definition and assessment of a practical quantum advantage. In *2023 IEEE International Conference on Quantum Software (QSW)*, page 162, 2023.
- [16] Timo Felser, Marco Trenti, Lorenzo Sestini, Alessio Giannele, Davide Zuliani, Donatella Lucchesi, and Simone Montangero. Quantum-inspired machine learning on high-energy physics data. *npj Quantum Inf*, 7:111, 2021.
- [17] Scott Aaronson. The learnability of quantum states. *Proc. R. Soc. Lond. A*, 463:3089, 2007.
- [18] Masahide Sasaki and Alberto Carlini. Quantum learning and universal quantum matching machine. *Phys. Rev. A*, 66:022303, Aug 2002.
- [19] Alessandro Bisio, Giulio Chiribella, Giacomo Mauro D’Ariano, Stefano Facchini, and Paolo Perinotti. Optimal quantum learning of a unitary transformation. *Phys. Rev. A*, 81:032324, Mar 2010.
- [20] Maria Schuld, Ilya Sinayskiy, and Francesco Petruccione. An introduction to quantum machine learning. *Contemporary Physics*, 56(2):172–185, 2015.
- [21] Jacob Biamonte, Peter Wittek, Nicola Pancotti, Patrick Rebentrost, Nathan Wiebe, and Seth Lloyd. Quantum machine learning. *Nature*, 549:195, 2017.
- [22] Kyriaki A. Tychola, Theofanis Kalampokas, and George A. Papakostas. Quantum machine learning — an overview. *Electronics*, 12(11), 2023.
- [23] Amine Zeguendry, Zahi Jarir, and Mohamed Quafafou. Quantum machine learning: A review and case studies. *Entropy*, 25(2), 2023.
- [24] Alexander Alodjants Alexey Melnikov, Mohammad Kordzanganeh and Ray-Kuang Lee. Quantum machine learning: from physics to software engineering. *Adv. Phys. X*, 8(1):2165452, 2023.
- [25] Tarun Dutta, Adrián Pérez-Salinas, Jasper Phua Sing Cheng, José Ignacio Latorre, and Manas Mukherjee. Single-qubit universal classifier implemented on an ion-trap quantum device. *Phys. Rev. A*, 106:012411, Jul 2022.
- [26] Takafumi Ono, Wojciech Roga, Kentaro Wakui, Mikio Fujiwara, Shigehito Miki, Hirotaka Terai, and Masahiro Takeoka. Demonstration of a bosonic quantum classifier with data reuploading. *Phys. Rev. Lett.*, 131, 2023.
- [27] Aleksei Tolstobrov, Gleb Fedorov, Shtefan Sanduleanu, Shamil Kadyrmetov, Andrei Vasenin, Aleksey Bolgar, Daria Kalacheva, Viktor Lubanov, Aleksandr Dorogov, Julia Zotova, Peter Shlykov, Aleksei Dmitriev, Konstantin Tikhonov, and Oleg V. Astafiev. Hybrid quantum learning with data re-uploading on a small-scale superconducting quantum simulator, arXiv:2305.02956, 2023.
- [28] Elena Peña Tapia, Giannicola Scarpa, and Alejandro Pozas-Kerstjens. A didactic approach to quantum machine learning with a single qubit. *Phys. Scr.*, 98, 2022.
- [29] Thien Nguyen, Daanish Arya, Marcus W. Doherty, Nils Herrmann, Johannes Kuhlmann, Florian Preis, Pat Scott, and Simon Yin. Software for massively parallel quantum computing. arXiv:2211.13355, 2022.
- [30] Philip Eason-McCaldin, Ahmed Bouridane, Ammar Belatreche, and Richard Jiang. On depth, robustness and performance using the data re-uploading single-qubit classifier. *IEEE Access*, 9:65127–65139, 2021.
- [31] Mariam Akhtar et. al. *in preparation*, 2024.
- [32] Marcus W. Doherty, Neil B. Manson, Paul Delaney, Fedor Jelezko, Jörg Wrachtrup, and Lloyd C.L. Hollenberg. The nitrogen-vacancy colour centre in diamond. *Phys. Rep.*, 528:1, 2013.